Structural and Electronic Characterizations of Two Isomers of Ce@C_{82}

Yoshie Rikiishi,[†,‡] Yoshihiro Kubozono,*[,†,‡] Tomoko Hosokawa,[†,‡] Kana Shibata,[†,‡] Yusuke Haruyama,[†,‡] Yasuhiro Takabayashi,[†,‡] Akihiko Fujiwara,[‡,§] Shinichiro Kobayashi,[‡,||] Satoshi Mori,[‡,||] and Yoshihiro Iwasa[‡,||]

Department of Chemistry, Okayama University, Okayama 700-8530, Japan, CREST, Japan Science and Technology Corporation, Kawaguchi, 332-0012, Japan, Japan Advanced Institute for Science and Technology, Ishikawa 923-1292, Japan, and Institute for Materials Research, Tohoku University, Sendai 980-8577, Japan

Received: January 15, 2004

X-ray diffractions and electronic transports for the Ce@C_{82} isomers I and II, which refer to major and minor isomers, respectively, are studied in a wide temperature region to clarify the structural and electronic properties characteristic of individual isomers. The X-ray diffraction patterns observed at 295 K can be indexed based on simple cubic (sc) structures with lattice constants, *a*'s, of 15.78(1) Å for isomer I and 15.74(4) Å for isomer II. Rietveld analyses are achieved for these X-ray diffraction patterns with a space group of $Pa\bar{3}$. Temperature dependence of *a* for isomer I shows a drastic change around 170 K, which implies existence of a structural phase transition. The structural phase transition above 300 K cannot be detected for Ce@C_{82} isomer I in contrast with La@C_{82} isomer I in which the phase transition at 400 K was detected by differential scanning calorimetry and dielectric constant measurements. The temperature dependence of *a* for isomer II indicates no structural phase transition from 100 to 300 K. The pressure dependence of *a* for isomer I exhibits a monotonic decrease with an increase in pressure. This result implies no pressure-induced structural phase transition for isomer I. The temperature dependence of resistivities for thin films of these isomers is studied by a four-probe method, and it shows narrow-gap semiconductor-like behaviors. The energy gaps of isomers I and II are 0.33 and 0.55 eV, respectively. The difference in the structural and electronic properties among the isomers of metallofullerenes will attract much interest in chemistry and materials science.

I. Introduction

The structures and electronic properties of isomer-separated solids in metallofullerenes have attracted special attention in chemistry as new spherical molecules and in materials science because of their possibilities of applications toward materials with novel functionalities. The crystal structures of metallofullerenes have been determined by Rietveld analyses for X-ray powder diffraction data. First, the crystal structure of 1:1 toluene solvate of Y@C_{82} was determined by combining maximum entropy method (MEM) and Rietveld analysis for the X-ray diffraction pattern.[1] The MEM density map obtained by the analysis showed a clear endohedral structure and displacement of Y from the C_{82} cage center. Subsequently, structural determinations of 1:1 toluene solvates of Sc@C_{82} and Sc_2@C_{84} were achieved by the same method as that for Y@C_{82}.[2,3] These crystals were monoclinic, and the space group was $P2_1$. These results also showed that Sc ions were encapsulated inside the cages. Furthermore, the charge transfer from Sc to the cage was found to be $+2.2e$ from the MEM density map. Recently, the endohedral structure for Sc_3N@C_{80} was confirmed by a single-crystal X-ray diffraction study of $(Sc_3N@C_{80})Co^{II}$-OEP$1.5CHCl_3 0.5C_6H_6$.[4] The average Sc−N distance was determined to be 2.069 Å. Sc_3N@C_{80} was different from other metallofullerenes studied so far in that the covalent bonds exist inside the cage. Furthermore, the structure of Sc_2@C_{66}, which did not satisfy the isolated pentagon rule (IPR), was determined by the MEM−Rietveld analysis.[5] This was the first example of metallofullerenes which did not follow IPR. These metallofullerenes are interesting materials in the chemistry of fullerenes because of the unique structures and electronic properties of the molecules.

On the other hand, the solvent-free solids of metallofullerenes are important from the viewpoints of solid-state chemistry and physics because novel physical properties should be realized in crystalline solids without solvents; impurities such as solvents generally disturb the physical properties. The crystal structure of solvent-free metallofullerene was first studied with a very small size of single crystals of La@C_{82} isomer I by Watanuki et al; isomer I refers to a major isomer of metal endohedral C_{82} (M@C_{82}; M, lanthanide ions).[6,7] The study showed that crystals of La@C_{82} isomer I took a face-centered cubic (fcc) lattice with a lattice constant, *a*, of 15.78 Å at 300 K. The structural transitions to various phases were found in the solvent-free La@C_{82} crystals. The various phases were realized by differences in molecular orientations of the C_{82} cages and the molecular electric dipole moment induced by displacement of La from the cage center: fcc at 180−300 K, rhombohedral at 140−180 K, triclinic at 20−140 K in slow cooling, and simple cubic (sc) at 20−132 K in rapid cooling. Two structural phase transitions around 150 and 400 K for the solvent-free La@C_{82} were reported based on the temperature dependence of differential scanning calorimetry (DSC) and the dielectric constant.[8] The structural transitions around 150 and 400 K were assigned to the second- and first-order phase transitions, respectively. Recently, the structure for the solvent-free solid of Dy@C_{82}

* To whom correspondence should be addressed.
† Okayama University.
‡ Japan Science and Technology Corp.
§ Japan Advanced Institute for Science and Technology.
|| Tohoku University.

10.1021/jp049787w CCC: $27.50
Published on Web 05/14/2004

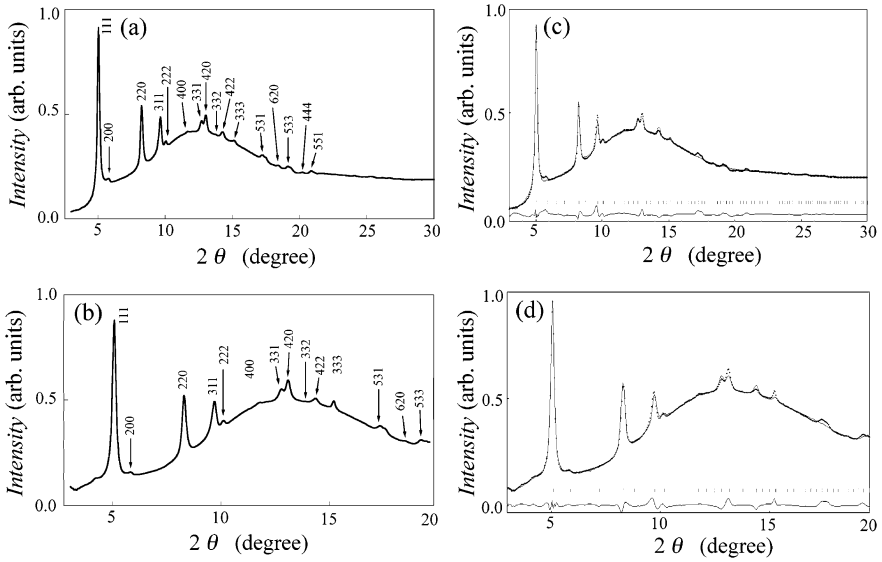

Figure 1. Observed X-ray diffraction patterns for the Ce@C_{82} isomer I at (a) 295 and (b) 50 K. The patterns calculated with the structural parameters determined by Rietveld refinement (—) and the observed patterns (+) at (c) 295 and (d) 50 K. Allowed peak positions and the difference between the observed and calculated patterns are drawn by tick (middle) and solid lines (bottom), respectively.

isomer I was studied by Rietveld analysis for the X-ray diffraction pattern, and the temperature and pressure dependences of a were also reported.[9,10] The cage symmetry of C_{82} in Dy@C_{82} isomer I was C_{2v}, and the crystal structure was not fcc but sc with a space group of $Pa\bar{3}$.[10] Subsequently, it was shown that crystals of solvent-free Ce@C_{82} isomer I were isomorphous with those of the Dy@C_{82} isomer I.[11] The value of a was 15.78(1) Å for isomers I of Dy@C_{82} and Ce@C_{82}.

We studied electronic properties of solvent-free solids of Dy@C_{82} and Ce@C_{82} and found that these materials were small-gap semiconductors with an energy gap, E_g, of 0.2−0.4 eV.[10,11] The field effect transistor (FET) with a thin film of Dy@C_{82} showed a normally on type property.[12] The normally on character originates from the small E_g. Thus, the FET device shows behaviors different from those of C_{60} and C_{70} FETs, showing normally off characters.[12] This suggests the possibility of development of electronic devices and materials based on the intrinsic natures of metallofullerens.

The difference in the crystal phases and physical properties has never been clarified among isomers of any metallofullerene. Even in the most popular metallofullerenes, M@C_{82}, the crystal phases and their structures have been studied only for the major isomer (isomer I). This originates from a difficulty in obtaining the minor isomers. Nevertheless, it is very important to know the structures and electronic properties of solids of individual isomers in order to select the most suitable isomer for realization of electronic devices and materials with high functionalities. Further, the correlations between the structures of the isomers and their electronic properties are very interesting as pure chemistry. In the present study, the structures of Ce@C_{82} isomers I and II, which refer to major and minor isomers, respectively, are studied by X-ray diffraction in a wide temperature and pressure region. This is the first report on crystal structures of both major and minor isomers of M@C_{82}. Furthermore, the electronic transports for thin films of the isomer-separated Ce@C_{82} have been studied for the first time in order to clarify the effect of the molecular symmetry on the physical properties.

II. Experimental Section

The isomer-separated samples, isomers I and II of Ce@C_{82}, were obtained by repeating a high-performance liquid chromatography (HPLC) as described elsewhere.[13] Characterization was performed by time-of-flight mass and UV−vis−NIR spectra. Isomer I sample contained no isomer II, but isomer II sample contained ~10% of isomer I. The solvent-free solids of isomers I and II were prepared according to the method described elsewhere.[9−11,13] The solid samples for X-ray diffraction measurements were introduced into glass capillaries (ϕ = 0.5 mm) in an Ar glovebox without exposure to air. The X-ray diffraction patterns for the isomers were measured with synchrotron radiation of λ = 0.8015(2) Å at BL-1B of KEK−PF. The Rietveld refinements of the X-ray diffraction pattern for isomers I and II were performed with the Rietan-2000 program developed by Izumi.[14]

Thin films of Ce@C_{82} isomers I and II were fabricated on four gold electrodes of SiO_2/Si substrates according to the procedure reported previously.[12] The thickness of the SiO_2 layer was 440 nm, and the channel length, L, was 50 μm. The thicknesses of thin films of Ce@C_{82} isomers I and II were determined by a surface profiler to be 420 and 170 nm, respectively. Furthermore, the widths of thin films of isomers I and II were 2000 μm. The resistivity, ρ, was measured by a four-probe method under ~10^{-4} Torr.

III. Results and Discussion

1. Structure of Isomer I. The X-ray diffraction pattern of Ce@C_{82} isomer I at 295 K can be indexed based on an sc lattice with a of 15.78(1) Å (Figure 1a). The value of a for Ce@C_{82} isomer I is the same as that found for Dy@C_{82} isomer I.[9,10] As shown in Figure 1b, the X-ray diffraction pattern at 50 K can also be indexed with an sc lattice, and a is 15.690(9) Å. Recently, we performed a preliminary Rietveld refinement for the X-ray diffraction pattern of the Ce@C_{82} isomer I at 295 K with a space group of $Pa\bar{3}$.[11] In the analysis, the molecular symmetry for isomer I was assumed to be C_{2v} and the C_2 axis of the molecule was aligned along [111] direction. The Ce ion was located near a six-membered ring on the C_2 axis based on the local structure around Ce determined from EXAFS.[15] This analysis resulted in a good agreement between the experimental and calculated patterns.[11] Furthermore, the Ce ion showed a large fluctuation around the C_2 axis.

In the present study, the Rietveld refinements for isomer I are extensively performed by assuming various molecular

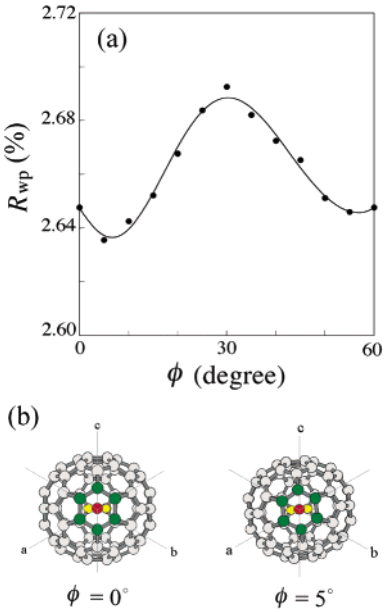

Figure 2. (a) Plot of R_{wp} vs ϕ in the Rietveld refinement for the X-ray diffraction pattern of isomer I at 295 K. (b) Molecular structures at $\phi = 0°$ and 5° for the Ce@C_{82} isomer I viewed along [111]. The green and yellow circles refer to the C atoms constituting the hexagon ring and the fused bond between two hexagon rings, respectively. The C_2 axis of the C_{2v}−C_{82} cage passes through the centers of green hexagon ring and yellow fused bond. The red circle refers to the Ce ion.

orientations and various positions of the Ce ions. The space group of $Pa\bar{3}$ requires a $\bar{3}$ around [111] in the unit cell. The molecule of isomer I must have an inversion disorder as well as a 3-fold ratchet-type disorder because the molecule possesses no $\bar{3}$ symmetry. In the unit cell, 82 C atoms occupy 24*d* site of the space group $Pa\bar{3}$ with an occupancy factor of 1/6. First, the Ce ion was placed on the C_2 axis of the molecule (8*c* site) with an occupancy of 1/2. This space group allows the molecule to rotate around [111]. The rotation angle around [111] is denoted by ϕ. The ϕ dependence of the weighted pattern *R* factor, R_{wp}, in the Rietveld refinement for the X-ray diffraction pattern at 295 K is shown in Figure 2a; the molecular orientation at $\phi = 0°$ is defined as shown in Figure 2b. A minimum R_{wp} of 2.64% is clearly observed at $\phi = 5°$. This result suggests that the molecule orients around $\phi = 5°$ as shown in Figure 2b, which is different from ϕ for Dy@C_{82} isomer I, 30°. The pattern calculated with the structures at $\phi = 5°$ is shown in Figure 1c. A good fit is seen between the experimental and calculated patterns (Figure 1c).

Furthermore, the Rietveld refinements were performed by changing the position of the Ce ion and the temperature factor, *B*. The plot of R_{wp} vs the distance of Ce ion from the cage center, r_{O-Ce}, is shown in Figure 3a, where the Ce ion is displaced from the cage center along the C_2 axis. This plot is symmetric because of the existence of inversion symmetry. The flat minimum in R_{wp} is observed within the displacement of ±2 Å, and the R_{wp} plot exhibits a small peak around r_{O-Ce} of 0 Å. This implies that the Ce ion can migrate within the cave of the C_{82} cage, and the Ce prefers the off-center position. Plots of R_{wp} vs r_{O-Ce} are shown in Figure 3b and c; here the Ce ion is placed on a 24*d* site and displaced from the cage center along two lines perpendicular to the C_2 axis. In the same manner as the case of the displacement along the C_2 axis (Figure 3a), the flat minima in R_{wp} are observed within r_{O-Ce} of ±2 Å in both plots shown in Figure 3b and c, and the R_{wp} plots exhibit small peaks around r_{O-Ce} of 0 Å. The minimum values of R_{wp} are

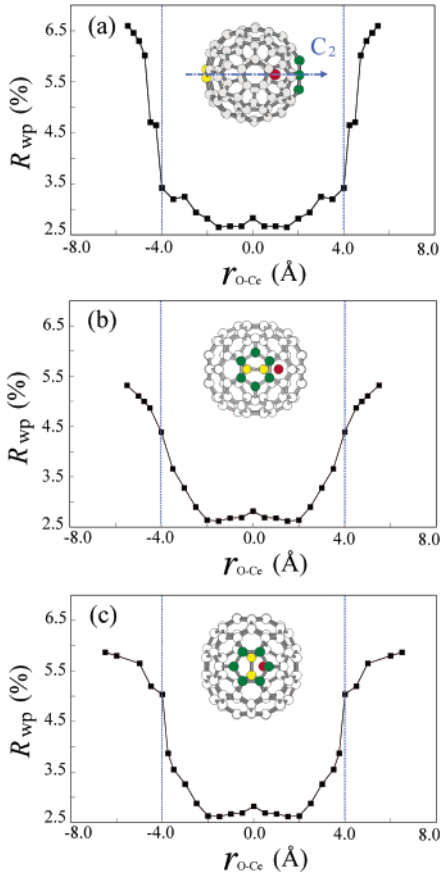

Figure 3. Plots of R_{wp} vs r_{Ce-O} in the Rietveld refinement for the X-ray diffraction pattern of isomer I at 295 K. (a) Ce ion is displaced along the C_2 axis, and (b and c) Ce ions are displaced along the lines perpendicular to the C_2 axis. The molecular structure is drawn in each graph so that the direction of displacement of Ce ions can be understood. (a−c) Dotted lines drawn in blue imply the molecular size of Ce@C_{82}. The green, yellow, and red circles indicate the hexagon ring, the fused bond, and the Ce ion, respectively.

almost the same in Figure 3a−c. These results show that the Ce ions can migrate around 2.0 Å from the cage center.

2. Temperature and Pressure Dependence of *a* in Isomer I. The temperature dependence of *a* in Ce@C_{82} isomer I is shown in Figure 4a. The value of *a* decreases slightly with a decrease in temperature from 295 to 170 K and shows a drastic decrease below 170 K. The values of *a* at 295 and 170 K are 15.78(1) and 15.75(3) Å, respectively, while the value of *a* at 140 K is 15.68(3) Å. The value of *a* is almost constant below 140 K. The drastic change in *a* below 170 K is an indication of a structural phase transition. The structural phase transition at 150−200 K is found in La@C_{82} from the temperature dependence of DSC and the dielectric constant.[8] Furthermore, the temperature dependence of *a* for Ce@C_{82} isomer I is similar to that found for isomer I of La@C_{82} from X-ray powder diffraction.[16]

Above 170 K the crystal structure was simple cubic with the space group of $Pa\bar{3}$. The molecule exhibits a ratchet-type disorder and inversion symmetry in the unit cell as described in section III.1. If only the inversion symmetry disappears below 150 K, the space group may change from $Pa\bar{3}$ to $P2_13$, which is a maximal subgroup of $Pa\bar{3}$. In this space group 3-fold symmetry around [111] is held. If the $\bar{3}$ symmetry disappears by freezing of both inversion and ratchet motions, the symmetry of the crystal lattice should be lower than the cubic lattice. The monoclinic lattice of $P2_1$ was found in the 1:1 toluene solvates of La@C_{82} and Sc@C_{82}.[2,17] In the crystals of toluene solvate,

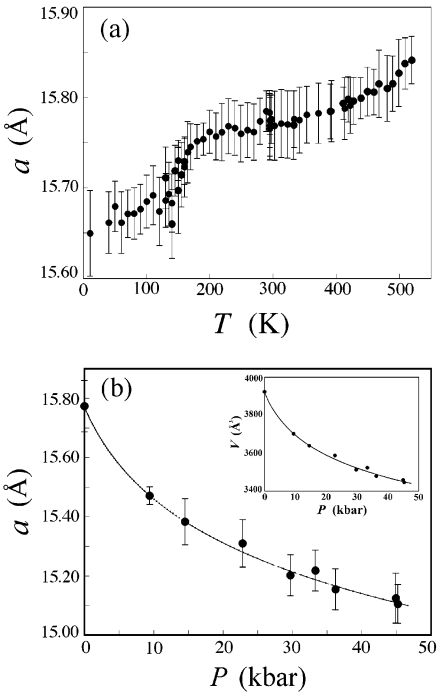

Figure 4. (a) Temperature and (b) pressure dependence of *a* for isomer I. The pressure dependence of *V* is shown in the inset of b.

the motion of the M@C_{82} molecules was suppressed by the solvent molecules and the suppression led to a lowering of the symmetry of crystals. Rietveld refinements were tried for the X-ray diffraction pattern at 50 K with space groups of $Pa\bar{3}$ and $P2_13$. The refinement with a space group of $Pa\bar{3}$ led to a better fit than that with $P2_13$ (Figure 1d). On the other hand, the refinement could not be achieved with a space group of $P2_1$; the atomic parameters of the C_{82} cage used in the refinement under $Pa\bar{3}$ and $P2_13$ were directly transferred to new parameters based on a space group of $P2_1$. Therefore, no clear lowering of the crystal symmetry was detected below 150 K. The value of *a* at 50 K is estimated to be 15.690(9) Å from Rietveld analysis with $Pa\bar{3}$ (Figure 1d).

The value of *a* for Ce@C_{82} isomer I increases monotonically above 300 K. No drastic change is observed in the temperature dependence of *a* around 400 K, in contrast to the case of La@C_{82}, where a clear structural phase transition was found from the temperature dependence of DSC and dielectric constant.[8] All X-ray diffraction peaks above 300 K can be indexed with an sc cell constant. The $a-T$ plot shows a slight deviation from the monotonic increase above 500 K. However, it cannot be concluded whether the deviation is associated with the structural phase transition.

The pressure dependence of *a* for isomer I at 295 K is shown in Figure 4b. The value of *a* decreases monotonically from $a = 15.78$ Å at 1 bar to 15.11(7) Å at 45 kbar. The plot can be fitted with *Murnagon* equation of states (EOS).[18,19] This result implies that no pressure-induced structural phase transition occurs at least up to 45 kbar at 295 K. The bulk modulas, K_0, is estimated to be 97 kbar from the *V* vs *p* plot shown in the inset of Figure 4b. K_0 is close to that, 95 kbar, of Dy@C_{82} estimated from the $V-P$ plot. This shows that the behavior under pressure is similar among M@C_{82}.

3. Structure and Its Temperature Dependence of Isomer II. The X-ray diffraction pattern of isomer II sample is shown in Figure 5a, which can be indexed with an sc structure as in isomer I. The value of *a* for isomer II is estimated to be 15.74(4) Å at 295 K. This value is almost the same as that, 15.78(1) Å, of isomer I. The molecular symmetry of Ce@C_{82} isomer II was suggested to be C_s from the similarity in the UV−vis−NIR spectrum to that for La@C_{82} isomer II;[11] the molecular symmetry of La@C_{82} isomer II was determined to be C_s from ^{13}C NMR data.[20]

In the present study, Rietveld analysis has been performed with a molecular structure of C_s(c) for Ce@C_{82} isomer II. The C_s(c) corresponds to the most stable structure determined theoretically for C_{82}^{3-} among three C_s-C_{82} structures which satisfy IPR.[21] Three C_s structures of the C_{82} cage are shown in Figure 6, and the notations a, b, and c follow those used in ref 21. We adopted the model that the Ce ion lies on the line which passes through the center of a six-membered ring and the center of a fused bond between two hexagon rings in the C_s(c)−C_{82} cage (Figures 5c and 6c). This line lies in a σ_h plane of the cage. The Ce ion was initially located near the center of the fused bond on the line. Very recently, this structure was confirmed by EXAFS.[15]

The space group of $Pa\bar{3}$ was adopted in the Rietveld refinement for isomer II. A line which passes through the center of a six-membered ring and the center of a fused bond in the C_s(c)−C_{82} cage was aligned along [111]. The space group of $Pa\bar{3}$ requires $\bar{3}$ symmetry around [111]. As this molecule has no $\bar{3}$ symmetry, the number of the independent C atoms is 82. All C atoms occupy 24*d* site, and the Ce ion is placed on the 8*c* site. The occupancies are 1/6 for the 24*d* site and 1/2 for the 8*c* site. In this space group, the cage of isomer II should have inversion symmetry and a 3-fold ratchet-type disorder to satisfy the $\bar{3}$ symmetry around [111].

The final Rietveld refinement for the X-ray diffraction pattern of this sample was performed by taking into consideration the existence of small amounts of isomer I in this sample, where the pattern of isomer I was calculated based on the structure described in section III.1. The fraction of isomer I determined by Rietveld refinement was ∼20%, whose value was substantially consistent with the fraction, ∼10%, estimated from the UV−vis−NIR spectrum of this sample. For isomer II of the main phase, the pattern was calculated with the molecular structure at $\phi = 0°$. The final calculated diffraction pattern is shown in Figure 5b together with the experimental diffraction pattern; R_{wp} was 4.07%. The molecular structure of isomer II used in the Rietveld refinement and the σ_h plane are shown in Figure 5c. The X-ray diffraction pattern of isomer II at 105 K is shown in Figure 5d, which can also be indexed with the sc structure. The value of *a* is estimated to be 15.77(4) Å, whose value is almost the same as that at 295 K.

The temperature dependence of *a* in Ce@C_{82} isomer II is shown in Figure 7. Though the values of *a* are a little scattered, significant variation is not found in this plot. This result shows no structural transition in isomer II from 100 to 300 K, which is different from the result of isomer I. In the present study, we have not collected the diffraction data below 100 K. Therefore, whether the structural phase transition in isomer II occurs below 100 K cannot be determined. Nevertheless, the X-ray diffraction results give fundamental information on the structural properties of isomer II, which have not been obtained so far.

4. Transport Properties of Isomers I and II of Ce@C_{82}. The temperature dependence of ρ for thin films of Ce@C_{82} isomers I and II are shown in Figure 8a and b, respectively. Both ρ values decrease exponentially with an increase in temperature. The ρ values for isomers I and II are 17 and 11 kΩ cm at 290 K, respectively. The ln ρ vs $1/T$ plots for isomers I and II are shown in the insets of Figure 8a and b, respectively. Both plots exhibit linear relationships. These results implies that

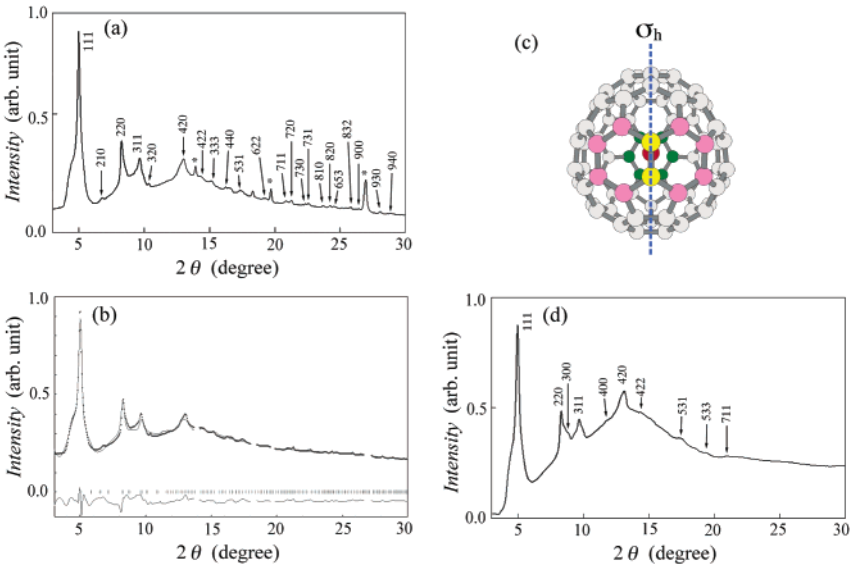

Figure 5. (a) Observed X-ray diffraction pattern for the Ce@C_{82} isomer II at 295 K, and (b) X-ray diffraction patterns observed (+) and calculated (−) with the structural parameters determined by Rietveld refinement. (b) Allowed peak positions and the difference between the observed and calculated patterns are drawn by tick (middle) and solid lines (bottom), respectively. The peak shown by an asterisk **(*)** could not be reproduced by the calculated pattern but is ascribable to sample holder. (c) Molecular structure of the C_s(c) isomer II. The yellow and pink circles refer to the C atoms constituting the fused bond between two hexagon rings and the remaining C atoms in the two hexagon rings, respectively. The green circles refer to the C atoms constituting the hexagon ring at the opposite side of the fused bond between the C atoms shown by yellow circles, and the red circle corresponds to the Ce ion. (d) Observed X-ray diffraction pattern for Ce@C_{82} isomer II at 105 K.

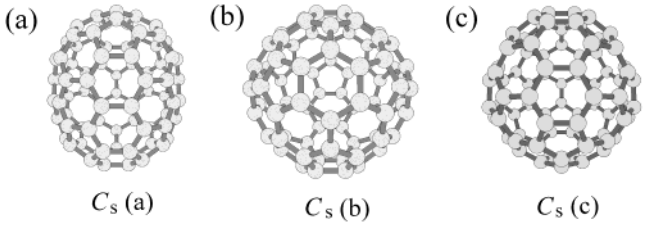

Figure 6. Three molecular structures of the C_s−C_{82} cage which satisfy IPR: (a) C_s(a), (b) C_s(b), and (c) C_s(c) structures predicted theoretically. The notations in parentheses are defined in ref 21.

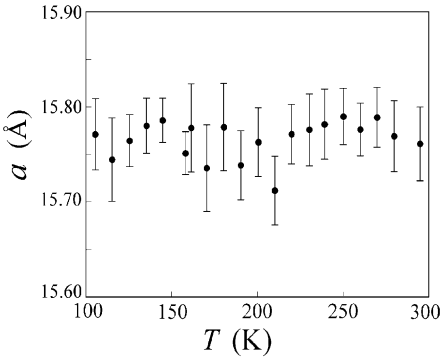

Figure 7. Temperature dependence of a in isomer II.

Ce@C_{82} isomers I and II are normal semiconductors. The values of E_g are estimated to be 0.33 eV for isomer I and 0.55 eV for isomer II. E_g, 0.4 eV, estimated previously for the isomer mixture of Ce@C_{82} is consistent with the mean value of E_g of these isomers.[11] These values are much smaller than those of C_{60} (1.8 or 2.1 eV) and C_{70} (2.2 eV).[22−24] The valence of the Ce ions in isomers of Ce@C_{82} was determined to be +3 based on the Ce−C_{82} stretching Raman peaks observed around 160 cm^{-1}.[11] This valence predicts metallic behavior for these isomers. Actually a theoretical calculation showed a metallic behavior for La@C_{82} (valence of La, +3) solids.[25] Nevertheless, electric transports showed semiconductor-like behaviors for isomers of Ce@C_{82} (Figure 8). This suggests that the electronic

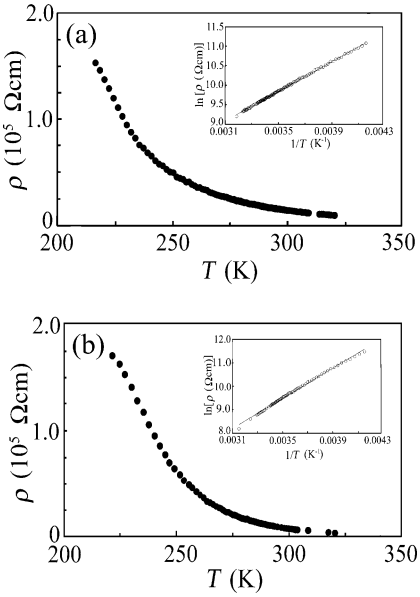

Figure 8. (a) Plots of ρ vs T for thin films of isomers (a) I and (b) II. The ln ρ vs. $1/T$ plots are shown in the insets.

repulsion energy, U, is large in trivalent metal endohedral C_{82} such as Ce@C_{82} because the large U should open an energy gap.

The field effect transistors (FETs) were tried to fabricate with thin films of Ce@C_{82} isomers I and II. The positive gate voltage, V_G, increased the drain current, I_D, while negative V_G decreased I_D. These results show that these devices operate as n-channel normally on depletion-type FETs. This result shows that the carrier in the channel conductance of the isomers of Ce@C_{82} is an electron, which is the same as the results of the fullerenes FETs fabricated so far, i.e., C_{60}, C_{70}, C_{84}, Dy@C_{82}, and La_2@C_{80} FETs.[12,26−28] The values of μ of the FETs with Ce@C_{82} isomers I and II were $\sim 10^{-4}$ cm^2 V^{-1} s^{-1}. The normally on character can be explained by the fact that values of E_g for the thin films of Ce@C_{82} isomers are very small as described above. In other

words, the high bulk currents of Ce@C_{82} isomers produce the normally on properties in these FETs. As the on/off ratios of these FET devices are extremely low at the present stage, further improvement of device performance is necessary for future application.

IV. Conclusion

The structures of two isomers of Ce@C_{82} have been determined by powder X-ray diffractions with synchrotron radiation. Both crystals showed simple cubic structures with a space group of $Pa\bar{3}$, and the values of a for both crystals were almost the same. The major isomer (I) of Ce@C_{82} showed a structural phase transition around 170 K, while the minor isomer (II) showed no structural transition from 100 to 300 K. A clear structural phase transition could not be observed for isomer I at the high-temperature region above 300 K, which is different from the La@C_{82} case. The pressure dependence of a in isomer I also showed no structural transition up to 50 kbar at 295 K. Rietveld refinements supported assignments of C_{2v} and C_s for the molecular symmetries of the C_{82} cage in isomers I and II, respectively. Rietveld refinements based on the models that the C_2 axis of the C_{2v}−C_{82} cage for isomer I and the axis passing the 6−6 fused bond and the center of the hexagon ring of C_s−C_{82} cage for isomer II align along [111] in the crystal lattices led to the good fits between the observed and calculated diffraction patterns, suggesting the validity of these structure models. Furthermore, it has been found that the Ce ion in isomer I can migrate far from the cage center by ±2 Å. In the present study, we studied the electronic transports of these isomers and found that the thin films of these isomers exhibited narrow-gap semiconductor-like behaviors. The values of E_g were 0.33 and 0.55 eV for isomers I and II, respectively. The FET devices of isomers I and II showed n-channel normally on properties, which are similar to those of Dy@C_{82} and C_{84} FET devices.[12,27] The normally on properties in the FET devices originate from small E_g's in the thin films of isomers I and II. The structures and electronic properties are similar between isomers I and II, but some properties, such as existence of structural phase transition and gap energy, observed from electric transports are different. The origin of the difference remains to be clarified, but development of materials and electronic devices based on the difference in structures and electronic properties between the isomers is a very exciting and challenging research subject in pure chemistry as well as materials science. The present study is the first step to develop new materials and devices with the isomer-separated metallofullerenes and opens a way to the chemistry of the isomers of metallofullerenes.

Acknowledgment. The X-ray diffraction study was performed under the proposal of KEK-PF, 2002G201. This work was supported by CREST of Japan Science and Technology Corp., by a Grant-in-Aid (15350089) from the Ministry of Education, Science, Sports and Culture of Japan, by Mitsubishi foundation, by Special Research Project and Joint Studies Program (2001−2003) of the Institute for Molecular Science, and by the Visiting Researcher's program Institute for Materials Research of Tohoku University (2003).

Supporting Information Available: CIF files. This material is available free of charge via the Internet at http://pubs.acs.org.

References and Notes

(1) Takata, M.; Umeda, B.; Nishibori, E.; Sakata, M.; Saito, Y.; Ohno, M.; Shinohara, H. *Nature* (*London*) **1995**, *377*, 46.

(2) Nishibori, E.; Takata, M.; Sakata, M.; Inakuma, M.; Shinohara, H. *Chem. Phys. Lett.* **1998**, *298*, 79.

(3) Takata, M.; Nishibori, E.; Umeda, B.; Sakata, M.; Yamamoto, E.; Shinohara, H. *Phys. Rev. Lett.* **1997**, *78*, 3330.

(4) Stevenson, S.; Rice, G.; Glass, T.; Harich, K.; Cromer, F.; Jordan, M. R.; Craft, J.; Hadju, E.; Bible, R.; Olmstead, M. M.; Maitra, K.; Fisher, A. J.; Balch, A. L.; Dorn, H. C. *Nature* **1999**, *401*, 55.

(5) Wang, C. R.; Kai, T.; Tomiyama, T.; Yoshida, T.; Kobayashi, Y.; Nishibori, E.; Takata, M.; Skata, M.; Shinohara, H. *Nature* **2000**, *408*, 426.

(6) Watanuki, T.; Fujiwara, A.; Ishii, K.; Matsuoka, Y.; Suematsu, H.; Ohwada, K.; Nakao, H.; Fujii, Y.; Kodama, T.; Kikuchi, K.; Achiba, Y. *AIP Conf. Proc.* **1999**, *CP486*, 124.

(7) Watanuki, T.; Fujiwara, A.; Ishii, K.; Matsuoka, Y.; Suematsu, H.; Ohwada, K.; Nakao, H.; Fujii, Y.; Kodama, T.; Kikuchi, K.; Achiba, Y. *Mol. Cryst. Liq. Cryst.* **2000**, *340*, 639.

(8) Nuttall, C. J.; Hayashi, Y.; Yamazaki, K.; Mitani, T.; Iwasa, Y. *Adv. Mater.* **2002**, *14*, 293.

(9) Takabayashi, Y.; Kubozono, Y.; Kanbara, T.; Fujiki, S.; Shibata, K.; Haruyama, Y.; Hosokawa, T.; Rikiishi, Y.; Kashino, S. *Phys. Rev. B* **2002**, *65*, 73405.

(10) Kubozono, Y.; Takabayashi, Y.; Shibata, K.; Kanbara, T.; Fujiki, S.; Kashino, S.; Fujiwara, A.; Emura, S. *Phys. Rev. B* **2003**, *67*, 115410.

(11) Shibata, K.; Rikiishi, Y.; Hosokawa, T.; Haruyama, Y.; Kubozono, Y.; Kashino, S.; Uruga, T.; Fujiwara, A.; Kitagawa, H.; Takano, T.; Iwasa, Y. *Phys. Rev. B* **2003**, *68*, 094104.

(12) Kanbara, T.; Shibata, K.; Fujiki, S.; Kubozono, Y.; Kashino, S.; Urisu, T.; Sakai, M.; Fujiwara, A.; Kumashiro, R.; Tanigaki, K. *Chem. Phys. Lett.* **2003**, *379*, 223.

(13) Iida, S.; Kubozono, Y.; Slovokhotov, Y.; Takabayashi, Y.; Kanbara, T.; Fukunaga, T.; Fujiki, S.; Emura, S.; Kashino, S. *Chem. Phys. Lett.* **2001**, *338*, 21.

(14) Izumi, F. In *The Rietveld Method*; Young, R. A., Ed.; Oxford University Press: Oxford, 1993; p 236.

(15) Takabayashi, Y.; Haruyama, Y.; Kubozono, Y.; Rikiishi, Y.; Hosokawa, T.; Shibata, K. *Chem. Phys. Lett.* **2004**, *388*, 23.

(16) Watanuki, T. Ph.D. Thesis, University of Tokyo, 1997.

(17) Nishibori, E.; Takata, M.; Sakata, M.; Tanaka, H.; Hasegawa, M.; Shinohara, H. *Chem. Phys. Lett.* **2000**, *330*, 497.

(18) Murnagham, F. D. *Proc. Natl. Acad. Sci. U.S.A.* **1947**, *30*, 244.

(19) Macdonald, J. R.; Powell, D. R. J. Res. *Natl. Bur. Stand., Sect. A* **1971**, *75*, 441.

(20) Akasaka, T.; Wakahara, T.; Nagase, S.; Kobayashi, K.; Waelchli, M.; Yamamoto, K.; Kondo, M.; Shirakura, S.; Maeda, Y.; Kato, T.; Kako, M.; Nakadaira, Y.; Gao, X.; Van Caemelbecke, E.; Kadish, K. M. *J. Phys. Chem. B* **2001**, *105*, 2971.

(21) Kobayashi, K.; Nagase, S. *Chem. Phys. Lett.* **1998**, *282*, 325.

(22) Takahashi, T.; Suzuki, S.; Morikawa, T.; Katayama-Yoshida, H.; Hasegawa, S.; Inokuchi, H.; Seki, K.; Kikuchi, K.; Suzuki, S.; Ikemoto, K.; Achiba, Y. *Phys. Rev. Lett.* **1992**, *68*, 1232.

(23) Kremer, R. K.; Rabenau, T.; Maser, W. K.; Kaiser, M.; Simon, A.; Haluska, M.; Kuzmany, H. *Appl. Phys. A* **1993**, *56*, 211.

(24) Han, B.-Y.; Hevesi, K.; Yu L.-M.; Gensterblum, G.; Rudolf, P.; Pireaux, J.-J.; Thiry, P. A.; Caudano, R. *J. Vac. Sci. Technol. A* **1995**, *13*, 1606.

(25) Amamiya, S.; Okada, S.; Suzuki, S.; Nakao, K. *Synth. Met.* **2001**, *121*, 1137.

(26) Haddon, R. C. *J. Am. Chem. Soc.* **1996**, *118*, 3041.

(27) Shibata, K.; Kubozono, Y.; Kanbara, T.; Hosokawa, T.; Fujiwara, A.; Ito, Y.; Shinohara, N. *Appl. Phys. Lett.* **2004**, *84*, 2572.

(28) Kobayashi, S.; Mori, S.; Iida, S.; Ando, H.; Takenobu, T.; Taguchi, Y.; Fujiwara, A.; Taninaka, A.; Shinohara, H.; Iwasa, Y. *J. Am. Chem. Soc.* **2003**, *125*, 8116.